1999

Two Amino Acids Within The A4 Helix Of Gα I1 Mediate Coupling With 5-Hydroxytryptamine 1B Receptors

Hyunsu Bae

Theresa M. Cabrera-Vera

Karyn M. Depree

Stephen G. Graber

Heidi E. Hamm

THE JOURNAL OF BIOLOGICAL CHEMISTRY
Vol. 274, No. 21, Issue of May 21, pp. 14963–14971, 1999
Printed in U.S.A.

Two Amino Acids within the α4 Helix of $G\alpha_{i1}$ Mediate Coupling with 5-Hydroxytryptamine$_{1B}$ Receptors*

(Received for publication, January 7, 1999, and in revised form, March 2, 1999)

Hyunsu Bae‡§, Theresa M. Cabrera-Vera‡, Karyn M. Depree¶, Stephen G. Graber¶, and Heidi E. Hamm‡‖

From the ‡Institute for Neuroscience, Northwestern University, Chicago, Illinois 60611 and the ¶Department of Pharmacology & Toxicology, West Virginia University, Morgantown, West Virginia 26506

We previously reported that residues 299–318 in $G\alpha_{i1}$ participate in the selective interaction between $G\alpha_{i1}$ and the 5-hydroxytryptamine$_{1B}$ (5-HT$_{1B}$) receptor (Bae, H., Anderson, K., Flood, L. A., Skiba, N. P., Hamm, H. E., and Graber, S. G. (1997) *J. Biol. Chem.* 272, 32071–32077). The present study more precisely defines which residues within this domain are critical for 5-HT$_{1B}$ receptor-mediated G protein activation. A series of $G\alpha_{i1}/G\alpha_t$ chimeras and point mutations were reconstituted with $G\beta\gamma$ and Sf9 cell membranes containing the 5-HT$_{1B}$ receptor. Functional coupling to 5-HT$_{1B}$ receptors was assessed by 1) [^{35}S]GTPγS binding and 2) agonist affinity shift assays. Replacement of the α4 helix of $G\alpha_{i1}$ (residues 299–308) with the corresponding sequence from $G\alpha_t$ produced a chimera (Chi22) that only weakly coupled to the 5-HT$_{1B}$ receptor. In contrast, substitution of residues within the α4-β6 loop region of $G\alpha_{i1}$ (residues 309–318) with the corresponding sequence in $G\alpha_t$ either permitted full 5-HT$_{1B}$ receptor coupling to the chimera (Chi24) or only minimally reduced coupling to the chimeric protein (Chi25). Two mutations within the α4 helix of $G\alpha_{i1}$ (Q304K and E308L) reduced agonist-stimulated [^{35}S]GTPγS binding, and the effects of these mutations were additive. The opposite substitutions within Chi22 (K300Q and L304E) restored 5-HT$_{1B}$ receptor coupling, and again the effects of the two mutations were additive. Mutations of other residues within the α4 helix of $G\alpha_{i1}$ had minimal to no effect on 5-HT$_{1B}$ coupling behavior. These data provide evidence that α4 helix residues in $G\alpha_i$ participate in directing specific receptor interactions and suggest that Gln^{304} and Glu^{308} of $G\alpha_{i1}$ act in concert to mediate the ability of the 5-HT$_{1B}$ receptor to couple specifically to inhibitory G proteins.

The interaction of heptahelical receptors with their cognate heterotrimeric guanine nucleotide-binding proteins (G proteins) represents an initial step in the transmission of extracellular signals across the plasma membrane (2–4). The receptor-G protein interaction modulates specific second messenger systems that result in a unique physiologic response to the extracellular signal. The particular downstream effect of G protein activation is not the result of an explicit interaction between each heptahelical receptor and a unique heterotrimeric G protein. On the contrary, G protein-coupled receptors have repeatedly been demonstrated to couple to several related members within the same family of G protein α subunits, albeit with differing levels of efficiency (5–11). Clawges *et al.* (12) demonstrated that the serotonin (5-HT)[1] 1B receptor couples to heterotrimers containing either $G\alpha_{i1}$, $G\alpha_{i2}$, $G\alpha_{i3}$, or $G\alpha_o$. Nevertheless, this receptor does not couple to heterotrimers containing another member of this same family, the $G\alpha_t$ subunit (12). Therefore, the 5-HT$_{1B}$ receptor represents one receptor system that can be exploited to investigate the precise molecular determinants governing selective receptor-G protein interactions.

Numerous biochemical studies have suggested that several subregions of $G\alpha$ (13–21) in addition to regions on $G\beta$ (20, 21) and $G\gamma$ (22–25) may act in concert to determine selective receptor-G protein interactions. The carboxyl-terminal domain of $G\alpha$ subunits, in particular, has been demonstrated to play a key role in eliciting several specific receptor-G protein interactions. However, the carboxyl-terminal regions of $G\alpha_{i1}$, $G\alpha_{i2}$, $G\alpha_{i3}$, and $G\alpha_t$ are highly homologous, and therefore, the carboxyl-terminal domain is not likely to be the primary determinant of 5-HT$_{1B}$ receptor-G protein selectivity between $G\alpha_{i/o}$ and $G\alpha_t$. The selectivity profile of the 5-HT$_{1B}$ receptor has facilitated the use of $G\alpha_i/G\alpha_t$ chimeras to map the residues that play a role in determining the specific interaction of the 5-HT$_{1B}$ receptor to inhibitory G proteins.

By using this approach, we previously demonstrated that substitution of the α4 helix and α4–β6 loop (amino acids 299–318) regions of $G\alpha_i$ with the respective sequence from $G\alpha_t$ markedly reduced the ability of this chimera to couple to the 5-HT$_{1B}$ receptor (1). These studies determined that the region corresponding to amino acids 299–318 in $G\alpha_{i1}$ plays a key role in determining the selective interaction between $G\alpha_{i1}$ and the 5-HT$_{1B}$ receptor (1). The intent of the present study was to define more precisely which amino acids within this domain are critical for selective 5-HT$_{1B}$ receptor coupling to inhibitory G proteins.

In addition to providing a useful model for receptor-G protein selectivity, the 5-HT$_{1B}$ receptor plays an important modulatory role in the central nervous system. 5-HT$_{1B}$ receptors are the primary terminal autoreceptors within the brain serotonin system (26). Activation of these receptors inhibits the release of

* This work was supported by National Institutes of Health Grant EY10291 (to H. E. H), American Heart Association Ohio-West Virginia Affiliate grant-in-aid (to S. G. G) and Research Fellowship Award 5T32CA70085-02 (to T. M. C.-V.).The costs of publication of this article were defrayed in part by the payment of page charges. This article must therefore be hereby marked "*advertisement*" in accordance with 18 U.S.C. Section 1734 solely to indicate this fact.

The atomic coordinates and structure factors (code 1TND) have been deposited in the Protein Data Bank, Brookhaven National Laboratory, Upton, NY.

‖ To whom correspondence should be addressed: Institute for Neuroscience, Northwestern University, 320 E. Superior, Searle Bldg., Rm. 5-555, Chicago, IL 60611. Tel.: 312-503-1109; Fax: 312-503-7345; E-mail: h-hamm@nwu.edu.

§ Current address: Dept. of Immunology and Infectious Diseases, Harvard School of Public Health, Boston, MA 02115.

[1] The abbreviations used are: 5-HT, 5-hydroxytryptamine; GTPγS, guanosine 5′-3-*O*-(thio)triphosphate; AMP-PNP, adenosine 5′-(β,γ imino)triphosphate; ANOVA, analysis of variance; CHAPS, 3-[(3-cholamidopropyl)dimethylammonio]-1-propanesulfonic acid.

5-HT into the synaptic cleft (27, 28). In addition, drugs that selectively interact with 5-HT_{1B} receptors have proven to be clinically useful for the treatment of migraine headache (29). Thus, deducing the molecular events that are essential to 5-HT_{1B} receptor-catalyzed G protein activation may aid our understanding of both normal and pathologic processes in brain serotonin systems.

By utilizing a series of $G\alpha_i/G\alpha_t$ chimeras coupled with site-directed mutagenesis, the present study reveals that α4 helical residues Gln^{304} and Glu^{308} of $G\alpha_{i1}$ are critical determinants of 5-HT_{1B} receptor coupling to inhibitory G proteins. This conclusion is supported by the observed marked reduction in receptor-catalyzed GDP/GTP exchange on $G\alpha_{i1}$ Q304K, E308L, and Q304K-E308L mutants. Moreover, whereas Gln^{304} and Glu^{308} are absolutely conserved among all $G\alpha_{i/o}$ isoforms, they are divergent between $G\alpha_{i/o}$ and $G\alpha_t$ subunits. The crystal structure of $G\alpha_i$ reveals that Gln^{304} and Glu^{308} are surface-exposed (30, 31), and mutation of these residues (Q304K and E308L) may alter the surface potential of the α subunit. Hence, these residues may interact directly with the 5-HT_{1B} receptor to mediate receptor coupling. Mutation of these residues may also indirectly influence the secondary structure of neighboring domains resulting in an inability of the 5-HT_{1B} receptor to couple to the mutant inhibitory α subunits.

EXPERIMENTAL PROCEDURES

Materials—Nucleotides and enzymes were purchased either from Boehringer Mannheim or from Amersham Pharmacia Biotech. Serotonin was obtained from Sigma. [^{35}S]GTPγS (1250 Ci/mmol) and [^{3}H]5-HT (22–30 Ci/mmol) were purchased from NEN Life Science Products.

Construction of Gα Mutant Genes—The present study used the *Escherichia coli* expression vectors $pHis_6G\alpha_{i1}$ or $pHis_6Chi3$ that contain a nucleotide sequence encoding a hexa-histidine tag under the control of a T7 promoter (32). *Bam*HI and *Hin*dIII digestion of $pHis_6Chi3$ released a 450-base pair DNA fragment corresponding to amino acid residues 214–354 of Chi3. This fragment was subcloned into pUC19 (pUC19-Chi3). To construct Chi22, Chi24, and Chi25, duplex oligonucleotides containing the desired mutations were ligated into the *Nae*I- and *Bgl*II-digested pUC19-Chi3. Sequences were confirmed, and the correct pUC19-based chimeras were cloned into the $pHis_6G\alpha_{i1}$ as a *Bam*HI and *Hin*dIII fragment. Generation of the *Bam*HI site in $pHis_6G\alpha_{i1}$ did not mutate any residues. Site-directed mutagenesis of either Chi22 or $G\alpha_{i1}$ was carried out using the QuikChange™ Site-directed Mutagenesis Kit (Stratagene, La Jolla, CA) according to the manufacturer's instructions. Either $pHis_6G\alpha_{i1}$ or $pHis_6Chi22$ served as the template for polymerase chain reaction-based mutagenesis.

Expression and Purification of $G\alpha_{i1}$ and Gα Mutants in E. coli—Hexa-histidine-tagged $G\alpha_{i1}$ or chimeric Gα subunits were expressed in *E. coli* BL21(DE3) cells and purified as described (32) with minor modification. Briefly, cell pellets were resuspended in buffer A (50 mM Tris-HCl, pH 8.0, 50 mM NaCl, 5 mM $MgCl_2$) supplemented with 50 μM GDP, 0.1 mM phenylmethylsulfonyl fluoride, and 5 mM β-mercaptoethanol, sonicated, and then centrifuged at 100,000 × *g* for 60 min. The supernatant was loaded onto a Ni^{2+}-nitrilotriacetic acid-agarose resin column (His-Bond, Novagen). Eluted samples were dialyzed overnight against buffer A in the presence of 20% glycerol, 0.1 mM phenylmethylsulfonyl fluoride, and 2 mM β-mercaptoethanol and then further purified by high performance liquid chromatography (Waters Protein-Pak QHR-15, Waters Chromatography). Protein concentrations were determined using the Coomassie Blue method (33) with bovine serum albumin (Pierce) as the standard.

Expression and Purification of G Protein Subunits—For affinity shift assays, the expression and purification of the G protein α subunits in Sf9 cells was performed as described (34, 35) except that the final chromatography step was performed on 15-micron Waters Protein-Pak QHR (Waters Chromatography). Recombinant $\beta_1\gamma_2$ subunits were purified from Sf9 cells using a His_6-γ_2 as described by Kozasa and Gilman (36). The native retinal βγ subunits used for the GTPγS binding experiment were purified as described (37).

Preparation of Sf9 Membranes Containing 5-HT_{1B}-expressed Receptors—Sf9 cells were infected with recombinant baculovirus containing cDNA for the 5-HT_{1B} receptor, cultured, and harvested as described (34). Membranes were prepared according to a previously published protocol (1). Briefly, harvested cells were thawed and resuspended in ice-cold homogenization buffer (10 mM Tris-HCl, pH 8.0, 25 mM NaCl, 10 mM $MgCl_2$, 1 mM EGTA, 1 mM dithiothreitol, 0.1 mM phenylmethylsulfonyl fluoride, 20 μg/ml benzamidine and 2 μg/ml each of aprotinin, leupeptin, and pepstatin A) and burst by N_2 cavitation. Cavitated cells were centrifuged at low speed; the supernatant was removed and then centrifuged at 28,000 × *g* for 30 min at 4 °C. The resulting pellets were resuspended in 5 mM NaHEPES, pH 7.5, containing 1 mM EDTA and supplemented with the aforementioned protease inhibitors. The membranes were washed twice and resuspended in the same buffer (1–3 mg of protein/ml).

Reconstitution of Receptors with Exogenous G Proteins—Frozen Sf9 membranes were reconstituted as described (1). Briefly, membranes were pelleted and resuspended in reconstitution buffer (5 mM Na-HEPES, pH 7.5, 100 mM NaCl, 5 mM $MgCl_2$, 1 mM EDTA, 500 nM GDP, 0.04% CHAPS). G protein subunits were diluted in the same buffer, and the mixture was incubated at 25 °C for 15 min and then held on ice. The reconstitution mixture was diluted with binding assay buffer as described (1).

[^{3}H]5-Hydroxytryptamine Binding Assay—[^{3}H]5-HT binding to 5-HT_{1B} receptors reconstituted with Gα and $G\beta_1\gamma_2$ was determined as described previously (1). To estimate receptor number in individual membrane preparations, the membranes were reconstituted with a large excess (5 μM) of G protein heterotrimers containing $G\alpha_{i1}$ and the 5-HT_{1B} receptors labeled with 1, 10, and 40 nM [^{3}H]5-HT. It has been shown that such reconstitution effectively converts all of the expressed receptors to a coupled, high affinity for agonist state (12). B_{max} values were estimated by nonlinear regression analysis with GraphPad PRISM of the specific binding data using a fixed value (0.62 nM) for the high affinity K_D (12). For affinity shift assays, high affinity binding to 5-HT_{1B} receptors was determined using a single concentration of [^{3}H]5-HT near the K_D value for the radioligand (0.8–1.3 nM).

5-HT_{1B} Receptor-stimulated GTPγS Binding Assay—A GTPγS binding assay was used to quantitate receptor-catalyzed GDP/GTP exchange on Gα subunits as described (1). Briefly, membranes were incubated with 1 mM AMP-PNP at 37 °C for 1 h, and receptor coupling was reconstituted with Gα and Gβγ subunits on ice in 70 μl of reaction buffer A (25 mM Hepes, pH 7.4, 5 mM $MgCl_2$, 1 mM EDTA, 100 mM NaCl, 1 mM dithiothreitol) for 30 min and then diluted with 200 μl of reaction buffer A containing 150 nM GDP and 60 nM GTPγS. The addition of 30 μl of [^{35}S]GTPγS (~7 × 10^6 cpm) initiated the reaction which was incubated at 25 °C. The following final concentrations were used for the GTPγS assay: 1.28 nM 5-HT_{1B}, 40 nM Gα, and 40 nM retinal βγ. For agonist activation, 1 μM of 5-HT was included. Aliquots (20 μl) were withdrawn at various times, and the reaction was terminated by filtration. Radioactivity retained on the filters was quantitated with a liquid scintillation counter. As the actual receptor densities and protein concentrations varied in different experiments, some degree of variation in the absolute level of GTPγS binding was observed. As rhodopsin can couple to either G_t or G_i heterotrimers with equal efficiency (32), GTPγS binding data were normalized to the percent of maximal binding that occurred after incubating samples for 30 min in the presence of an excess amount (500 nM) of light-activated rhodopsin.

Fluorescence Assay—To ensure that recombinant Gα proteins are properly folded, instrinsic fluorescence of the subunits was measured as described (1, 32). Briefly, the AlF_4^--dependent conformational changes of activated Gα subunits were monitored by intrinsic tryptophan fluorescence changes with excitation at 280 nm and emission at 340 nm. The relative increase in fluorescence of 200 nM Gα subunits was determined from absorbance readings before and after the addition of 10 mM NaF and 20 μM $AlCl_3$.

Statistics—Affinity shift activity data and the initial rates of GDP/GTP exchange (Table I) were analyzed separately using a one-way analysis of variance (ANOVA). Differences between groups were determined by a Newman Keuls' *post hoc* test only after the ANOVA yielded a significant main effect.

RESULTS

The ability of 5-HT_{1B} receptors to couple selectively to heterotrimers containing members of the $G\alpha_{i/o}$ family of G proteins (12) facilitated the use of a series of $G\alpha_i/G\alpha_t$ chimeras to determine which amino acids within $G\alpha_i$ mediate this specific interaction. By using this approach, we previously demonstrated that $G\alpha_{i1}$ amino acid residues 299–318 (corresponding to the α4 helix and α4-β6 loop regions of $G\alpha_{i1}$) play a major role in determining the selective interaction with the 5-HT_{1B} receptor (1). Additional residues in the amino-terminal domain of $G\alpha_{i1}$

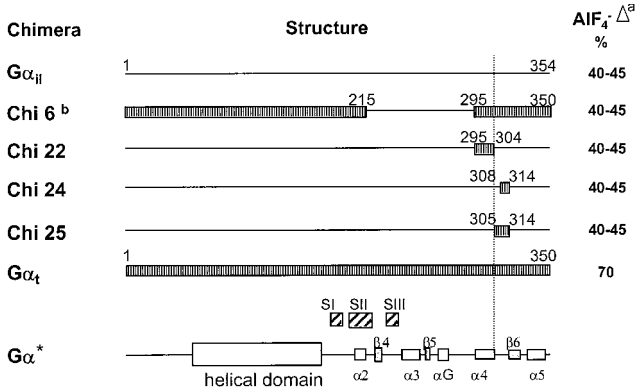

FIG. 1. **Secondary structure and AlF_4^--dependent tryptophan fluorescence change of Gα subunits.** *Numbers above* the wild type forms of $G\alpha_{i1}$ and $G\alpha_t$ represent the corresponding residues in each respective α subunit. *Numbers above* chimeric structures indicate the junction points of $G\alpha_t$ and $G\alpha_{i1}$ sequences and refer to amino acid positions in $G\alpha_t$. *, diagram of secondary structural domains common to Gα subunits. *SI, SII,* and *SIII* refer to the switch regions of Gα. [a] Percent increase in tryptophan fluorescence in the presence of 10 mM NaF and 20 μM $AlCl_3$ compared with basal (see "Experimental Procedures" for detail). The increase in tryptophan fluorescence indicates that all constructs were capable of undergoing conformational change in the presence of AlF_4^-. [b] As full-length $G\alpha_t$ is not easily expressed or purified, this $G\alpha_{i1}/G\alpha_t$ chimera was generated previously, crystallized, and shown to exhibit α_t-like coupling activity (32, 51).

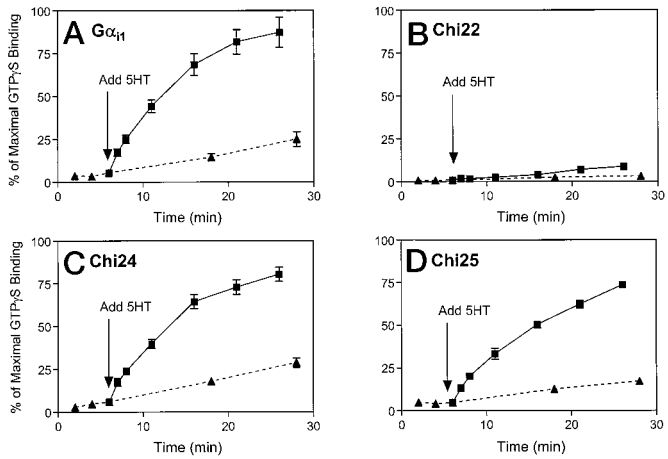

FIG. 2. **Time-dependent 5-HT_{1B} receptor-catalyzed GDP/GTP exchange on $G\alpha_{i1}$ and $G\alpha_{i1}/G\alpha_t$ chimeras.** Membranes expressing the 5-HT_{1B} receptor were reconstituted with either 40 nM $G\alpha_{i1}$ (*A*), Chi22 (*B*), Chi24 (*C*), or Chi25 (*D*) in the presence of 40 nM $\beta_1\gamma_1$. Data are expressed as the percentage of maximal GTPγS binding obtained in the presence of excess (500 nM) light-activated rhodopsin. *Squares* indicate GTPγS binding in the presence of 1 μM 5-HT (added at the 8.5-min time point), and *triangles* indicate the binding in the absence of agonist. Data represent the mean ± S.E. from three independent experiments.

were also determined to play a secondary role in 5-HT_{1B} receptor coupling (1).

The α4 Helical Domain of $G\alpha_{i1}$ Mediates the Ability of the 5-HT_{1B} Receptor to Couple to Inhibitory G Proteins—The present study initially used the same approach described above to identify which subdomain within this stretch of amino acids ($G\alpha_{i1}$ 299–318) is critical for functional 5-HT_{1B} receptor coupling to inhibitory G proteins. As shown schematically in Fig. 1, three chimeric $G\alpha_i/G\alpha_t$ proteins were generated in which either the α4 helix (Chi22) or portions of the α4–β6 loop region (Chi24 and Chi25) of $G\alpha_{i1}$ were replaced with the corresponding sequence from $G\alpha_t$. Prior to the assessment of coupling activity, the ability of each chimeric Gα subunit to bind GDP and undergo conformational change upon binding to GTP was tested by determining if the proteins undergo an AlF_4^--dependent increase in tryptophan fluorescence (32). This assay is based on the ability of AlF_4^-, which mimics the γ-phosphate of GTP, to induce the active conformation, which then results in an increase in intrinsic fluorescence of Trp^{211} in $G\alpha_{i1}$. Tryptophan fluorescence of all mutants and $G\alpha_{i1}$ used in this study increased 40–45% upon the addition of AlF_4^- (Fig. 1), consistent with our previous results (1, 32).

Functional coupling between the 5-HT_{1B} receptor and the chimeric proteins was assessed by examining both the ability of the 5-HT receptor agonist, serotonin, to stimulate receptor-catalyzed GDP/[^{35}S]GTPγS exchange on the α subunit, and the ability of the chimeric protein to induce the high affinity agonist binding state of the receptor (affinity shift activity). The underlying principle of the affinity shift assay is that activated receptors can be converted to a high affinity agonist binding state by the appropriate G protein heterotrimers (12). By using a low concentration of agonist near the K_D for the high affinity state and well below the K_D for the low affinity state, the formation of a functional agonist-receptor-G protein complex is readily detected as an enhanced level of ligand binding. This assay can detect changes in coupling with either native or recombinant receptor and G protein preparations (12, 38–40).

As shown in Fig. 2*A*, 5-HT stimulation of the 5-HT_{1B} receptor results in a time-dependent increase in [^{35}S]GTPγS binding to recombinant $G\alpha_{i1}$. Substitution of the α4 helix of $G\alpha_{i1}$ with the corresponding sequence from $G\alpha_t$ (Chi22) dramatically reduces (−90%) the ability of the 5-HT_{1B} receptor to couple to the chimeric G protein, as indicated by a marked reduction in the ability of 5-HT to stimulate [^{35}S]GTPγS binding to the Chi22 α subunit (Fig. 2*B* and Table I). In contrast, substitution of the α4–β6 loop $G\alpha_{i1}$ residues 308–314 with the corresponding region from $G\alpha_t$ (Chi24) failed to alter serotonin-stimulated receptor-catalyzed incorporation of [^{35}S]GTPγS into the chimeric α subunits (Fig. 2*C* and Table I). Interestingly, an overlapping chimera, Chi25, with $G\alpha_i$ residues 305–314 substituted with the corresponding $G\alpha_t$ residues shows a modest (28%) but significant ($p < 0.05$) reduction in the initial rate of GDP/GTP exchange (Table I).

The coupling ability of these same chimeras (Chi22, Chi24, and Chi25) was also examined by agonist affinity shift activity. Consistent with the [^{35}S]GTPγS experiments, the affinity shift activity of Chi22 was significantly reduced (−53%) in comparison to recombinant $G\alpha_{i1}$ (Fig. 3 and Table I). Likewise, as expected from the GTPγS data, the affinity shift activity of Chi24 did not significantly differ from $G\alpha_{i1}$. In contrast, although the affinity shift activity of Chi25 was reduced by 22%, this reduction did not reach statistical significance (Table I, Fig. 3). Taken together, these results localized the major molecular elements underlying the selective interaction of the 5-HT_{1B} receptor with $G\alpha_{i1}$ to the α4 helical domain.

Amino Acid Residues Gln^{304} and Glu^{308} of $G\alpha_i$ Are Critical Determinants of Coupling to 5-HT_{1B} Receptors—In order to map more precisely the specific amino acids that are critical for 5-HT_{1B} receptor coupling to $G\alpha_{i1}$, systematic site-directed mutagenesis studies were conducted based on either Chi22 or $G\alpha_{i1}$ (Fig. 4). Within Chi22 there are 5 residues that are divergent between $G\alpha_{i1}$ and $G\alpha_t$: $G\alpha_{i1}$-A300G, A301N, Q304K, C305V, and E308L (Fig. 4). Previous studies demonstrated that mutation of $G\alpha_{i1}$ residue Ala^{300} to glycine did not impair coupling to the 5-HT_{1B} receptor (1). Therefore, the present studies focused only on divergent residues between $G\alpha_{i1}$301 and $G\alpha_{i1}$308. The aim of the substitutions within Chi22 was to determine whether coupling to the 5-HT_{1B} receptor could be restored by replacing $G\alpha_t$ residues individually or in combination with the corresponding residues from $G\alpha_{i1}$. Mutants based on Chi22 (Chi22-N297A, Chi22-K300Q, Chi22-V301C, Chi22-L304E,

TABLE I

Affinity shift activity and initial rates of GDP/GTP exchange

Affinity shift data represent the means ± S.E. from 3 to 18 independent experiments. Initial rate data represent the means ± S.E. from 3 independent experiments. Affinity shift and initial rate data were analyzed separately using a one-way analysis of variance followed by a Newman Keuls' *post hoc test*.

Gα$_{i1}$ mutants	Affinity shift[a]	Initial rate[b]	Chimeras and Chi22 mutants	Affinity shift[a]	Initial rate[b]
Gα$_{i1}$	3.95 ± 0.20	870 ± 74.6	Chi24	3.63 ± 0.43	756 ± 53.5
Gα$_{i1}$-A301N	4.90 ± 0.32	977 ± 40.6[c]	Chi25	3.06 ± 0.44	629 ± 41.5[c]
Gα$_{i1}$-C305V	4.88 ± 0.14	846 ± 49.8	Chi22	1.86 ± 0.14[c]	88 ± 7.3[c]
Gα$_{i1}$-Q304K	4.51 ± 0.13	463 ± 32.7[c]	Chi22-N297A	1.97 ± 0.16[c]	40 ± 26.8[c]
Gα$_{i1}$-Q304K-C305V	4.03 ± 0.22	465 ± 32.4[c]	Chi22-V301C	2.71 ± 0.01	67 ± 6.5[c]
Gα$_{i1}$-E308L	3.45 ± 0.43	261 ± 18.8[c]	Chi22-K300Q	2.65 ± 0.16	215 ± 17.6[c,d]
Gα$_{i1}$-C305V-E308L	3.73 ± 0.43	261 ± 23.8[c]	Chi22-L304E	3.19 ± 0.25[d]	382 ± 33.3[c,d]
Gα$_{i1}$-Q304K-E308L	3.18 ± 0.38	140 ± 13.9[c,e]	Chi22-K300Q-L304E	4.51 ± 0.29[d,g]	799 ± 35.2[d,f]

[a] Affinity shift activities refer to the -fold enhancement above buffer controls of high affinity [^{3}H]5-HT binding to 5-HT$_{1B}$ receptors reconstituted with G protein heterotrimers containing the indicated α subunits.

[b] Initial rates of GDP/GTP exchange were calculated from the binding curves (Fig. 5*A* and Fig. 6*A*) and expressed as pmol of GTPγS bound per mole of protein per s.

[c] Significantly different than corresponding Gα$_{i1}$ value ($p < 0.05$).

[d] Chi22 mutants which are significantly greater than corresponding Chi22 value ($p < 0.05$).

[e] Significantly lower than Gα$_{i1}$-Q304K initial rate value ($p < 0.05$).

[f] Significantly greater than Chi22-K300Q and Chi22-L304E ($p < 0.05$).

[g] Chi22 mutant with an affinity shift value which is significantly different than Chi22-K300Q and Chi22-V301C ($p < 0.05$).

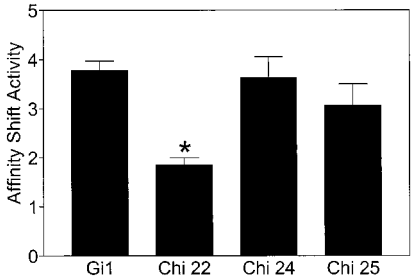

FIG. 3. **Affinity shift activity of Gα$_{i1}$/Gα$_t$ chimeras with 5-HT$_{1B}$ receptors.** Affinity shift activities refer to the -fold enhancement above buffer controls of high affinity [^{3}H]5-HT binding to 5-HT$_{1B}$ receptors reconstituted with G protein heterotrimers containing the indicated α subunits. Data represent the mean ± S.E. from 5 to 9 independent determinations using three separate membrane preparations where 5-HT$_{1B}$ receptors were expressed between 5.2 and 11.7 pmol/mg membrane protein. Exogenous G proteins were 1.3–3.3 μM during reconstitution and 45–112 nM during the binding assays which was a 35–50-fold molar excess over receptors. The concentration of [^{3}H]5-HT was 0.8–1.3 nM in all experiments. Data were analyzed using a one-way ANOVA followed by a Newman Keuls' *post hoc* test as described under "Experimental Procedures." *, significantly lower than Gα$_{i1}$ ($p < 0.05$).

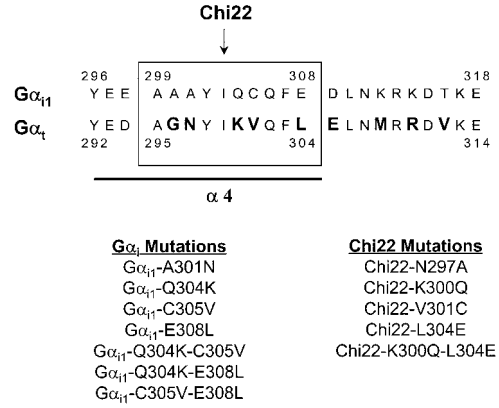

FIG. 4. **Primary sequence alignment of the α4–α4/β6 loop region of bovine Gα$_{i1}$ (residues 296–318) and Gα$_t$ (residues 292–314).** *Numbers immediately above* the primary sequence of Gα$_{i1}$ correspond to residues in Gα$_{i1}$. *Numbers immediately below* the primary sequence of Gα$_t$ correspond to residues in Gα$_t$. The *box* indicates the region of Gα$_{i1}$ that was substituted with the corresponding sequence from Gα$_t$ to generate Chi22. *Boldface letters* indicate residues within Gα$_t$ which diverge from Gα$_{i1}$ residues. Single or double mutations of Gα$_{i1}$ or Chi22 are listed *below* the sequence alignment.

and Chi22-K300Q-L304E) demonstrated varying degrees of receptor-catalyzed GDP/GTP exchange (Fig. 5*A* and Table I) and affinity shift activity (Fig. 5*B* and Table I). Similar to Chi22, Chi22-N297A exhibited only very weak coupling to the 5-HT$_{1B}$ receptor as exemplified both by the low levels of agonist-stimulated GTPγS binding (Fig. 5*A,* Table I) and by the low affinity shift activity of the mutant chimeras (Fig. 5*B*). Mutation of valine 301 to cysteine in Chi22 clearly failed to elevate the initial rate of GTPγS binding above Chi22 (Table I and Fig. 5*A*). Likewise, the affinity shift activity of this mutant did not significantly differ from Chi22. Mutants Chi22-K300Q and Chi22-L304E exhibited significant ($p < 0.05$) 2–4-fold increases in agonist-stimulated GDP/GTP exchange in comparison to the parent Chi22 (Table I). Consistent with these data, enhanced 5-HT$_{1B}$ receptor coupling was also observed with Chi22-L304E as measured by a significant 72% increase in the affinity shift activity over Chi22 (Fig. 5*B*). Although Chi22-K300Q caused a 42% increase in affinity shift activity over that observed for Chi22, this increase did not reach statistical significance. The critical nature of residues Gln^{304} and Glu^{308} is supported by the observation that the double mutant Chi22-K300Q-L304E completely restored GDP/GTP exchange *and* affinity shift activity to wild type Gα$_{i1}$ levels (Fig. 5 and Table I).

To confirm and further support the contention that Gα$_i$ residues Gln^{304} and Glu^{308} are particularly important determinants of 5-HT$_{1B}$ receptor coupling, single or double mutations were constructed in Gα$_{i1}$ (A301N, Q304K, C305V, and E308L). The aim of these experiments was to determine whether coupling to the 5-HT$_{1B}$ receptor could be reduced or eliminated by replacing these specific Gα$_{i1}$ residues with the corresponding residues from Gα$_t$. As illustrated in Fig. 6*A* and Table I, the single amino acid substitution Gα$_{i1}$-E308L markedly (−70%) and significantly ($p < 0.05$) reduced agonist-mediated stimulation of GTPγS binding to the mutant α subunit. Likewise, mutation Gα$_{i1}$-Q304K resulted in a moderate (>40%; $p < 0.05$) reduction in agonist-mediated GTPγS binding in comparison to recombinant Gα$_{i1}$. Consistent with these data, the double mutant Gα$_{i1}$-Q304K-E308L exhibited an even greater reduction in agonist-mediated GTPγS binding than either single mutation alone (Fig. 6*A* and Table I). Gα$_{i1}$-C305V did not significantly alter coupling to the 5-HT$_{1B}$ receptor as evidenced by the lack of effect on agonist-stimulated GDP/GTP exchange with this mutant (Table I). Quite unexpectedly, Gα$_{i1}$-A301N resulted in a small (+12%) but statistically significant ($p < 0.05$) increase in the initial rate of GDP/GTP exchange in comparison to Gα$_{i1}$ (Table I). In contrast to the marked reductions in [^{35}S]GTPγS

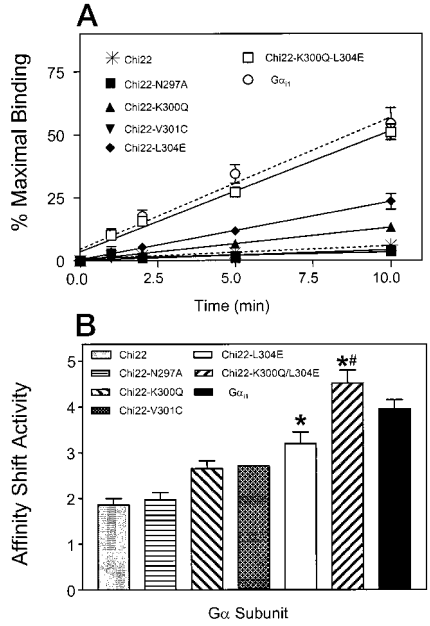

FIG. 5. **Functional coupling of the 5-HT_{1B} receptor to Chi22 mutants.** Membranes expressing the 5-HT_{1B} receptor were reconstituted with the indicated Chi22 mutants and $\beta\gamma$ subunits. *A* illustrates 5-HT_{1B} receptor-catalyzed GDP/GTP exchange on Chi22 point mutants. Data are expressed as the percentage of maximal GTPγS binding obtained in the presence of excess (500 nM) light-activated rhodopsin. *Curves* depict the difference between the rates of GTPγS binding in the presence and absence of 1 μM 5-HT. Data shown represent the mean ± S.E. of three independent experiments. The initial rates of nucleotide exchange calculated from these data are shown in Table I. *B* depicts the affinity shift activity of Chi22 mutants with 5-HT_{1B} receptors. Affinity shift activities refer to the -fold enhancement above buffer controls of high affinity [^{3}H]5-HT binding to 5-HT_{1B} receptors reconstituted with G protein heterotrimers containing the indicated α subunits. Data represent the mean ± S.E. from 3 to 9 independent determinations using three separate membrane preparations where 5-HT_{1B} receptors were expressed between 5.2 and 11.7 pmol/mg membrane protein. Exogenous G proteins were 1.3–3.3 μM during reconstitution and 45–112 nM during the binding assays which was a 35–50-fold molar excess over receptors. The concentration of [^{3}H]5-HT was between 0.8 and 1.3 nM in all experiments. Data were analyzed using a one-way ANOVA followed by a Newman Keuls' *post hoc* test as described under "Experimental Procedures." *, significantly greater than Chi22 ($p < 0.05$); #, significantly greater than Chi22-K300Q.

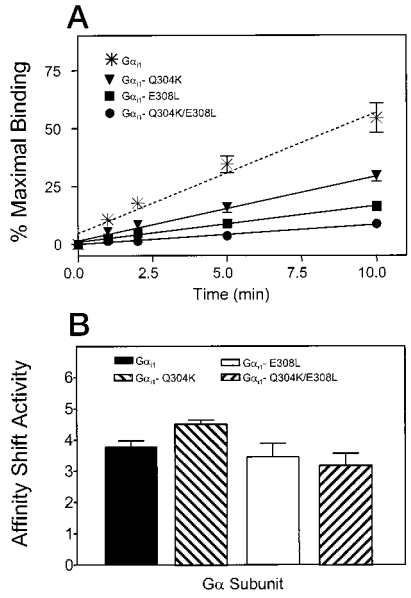

FIG. 6. **Functional coupling of the 5-HT_{1B} receptor to $G\alpha_{i1}$ mutants.** Membranes expressing the 5-HT_{1B} receptor were reconstituted with the indicated $G\alpha_{i1}$ mutants and $\beta\gamma$ subunits. *A* illustrates 5-HT_{1B} receptor-catalyzed GDP/GTP exchange on $G\alpha_{i1}$ point mutants. Data are expressed as the percentage of maximal GTPγS binding obtained in the presence of excess (500 nM) light-activated rhodopsin. *Curves* depict the difference between the rates of GTPγS binding in the presence and absence of 1 μM 5-HT. Data shown represent the mean ± S.E. of three independent experiments. The initial rates of nucleotide exchange calculated from these data are shown in Table I. *B* depicts the affinity shift activity of $G\alpha_{i1}$ mutants with 5-HT_{1B} receptors. Affinity shift activities refer to the -fold enhancement above buffer controls of high affinity [^{3}H]5-HT binding to 5-HT_{1B} receptors reconstituted with G protein heterotrimers containing the indicated α subunits. Data represent the mean ± S.E. from 3 to 6 independent determinations using 2 separate membrane preparations where 5-HT_{1B} receptors were expressed between 5.2 and 11.7 pmol/mg membrane protein. Exogenous G proteins were 1.3–3.3 μM during reconstitution and 45–112 nM during the binding assays which was a 35–50-fold molar excess over receptors. The concentration of [^{3}H]5-HT was between 0.8 and 1.3 nM in all experiments. Data were analyzed using a one-way ANOVA followed by a Newman Keuls' *post hoc* test as described under "Experimental Procedures." There were no significant differences between the affinity shift activity of $G\alpha_{i1}$ and those of the mutant Gα subunits.

binding observed with $G\alpha_{i1}$ mutants E308L, Q304K, and Q304K-E308L, no significant differences in affinity shift activities were observed between these mutants and $G\alpha_{i1}$ (Table I and Fig. 6*B*). Affinity shift activity also did not significantly vary between $G\alpha_{i1}$ and $G\alpha_{i1}$-A301N, C305V, or C305V/E308L (Table I).

This lack of correspondence between affinity shift activity and [^{35}S]GTPγS binding data for the $G\alpha_{i1}$ mutants is likely to result from differences in the sensitivity of these assays stemming from technical aspects involved in these measures. For example, the initial exchange rates (Table I) are determined from linear regression analysis of the [^{35}S]GTPγS binding data generated over the course of 10 min following the introduction of agonist to the assay (see Figs. 5*A* and 6*A*) with saturation of [^{35}S]GTPγS binding occurring by 30 min (Fig. 2*A*). In contrast, as is required for radioligand binding assays, the affinity of [^{3}H]5-HT for the 5-HT_{1B} receptor is determined only after equilibrium is reached (*i.e.* following a 1.5-h incubation with the agonist) and in the absence of GTP. Therefore, if GDP release is *impaired* in the $G\alpha_{i1}$ mutants (as would be suggested by alterations in [^{35}S]GTPγS binding) but not *prevented*, sufficient GDP could be released over the course of the experiment (1.5 h) such that at equilibrium the amount of high affinity receptors present in the preparation is similar for both $G\alpha_{i1}$ and the $G\alpha_{i1}$ mutants. Alternatively, the divergence between affinity shift activity and [^{35}S]GTPγS binding for the $G\alpha_{i1}$ mutants may be indicative of a change in GTPγS binding in the absence of a change in GDP release. This situation could only arise if GTPγS binding (rather than GDP release) has become the rate-limiting step as a result of the $G\alpha_{i1}$-Q304K and $G\alpha_{i1}$-E308L mutations. If this were the case, we might expect to observe this same phenomenon with the Chi22-K300Q, Chi22-L304E, and Chi22-K300Q-L304E mutants, which we do not. Therefore, although the studies herein do not preclude the possibility of changes in GTPγS binding in the absence of a change in GDP release, further studies will be required to assess the likelihood of this potential outcome.

Nonetheless, despite the variations between the affinity shift data and the GDP/GTP exchange rates for the $G\alpha_{i1}$ mutants, the affinity shift activity appeared to show overall trends in the same direction as the [^{35}S]GTPγS binding data. We, therefore, determined whether there was a correlation between affinity shift activity and the initial rates of GDP/GTP exchange as measured by [^{35}S]GTPγS binding. Fig. 7 illustrates the correlative comparison between these two data sets. Correlation analysis yielded a Pearson correlation coefficient of 0.80, indicating a significant correlation between the GDP/GTP exchange rate and the affinity shift activity.

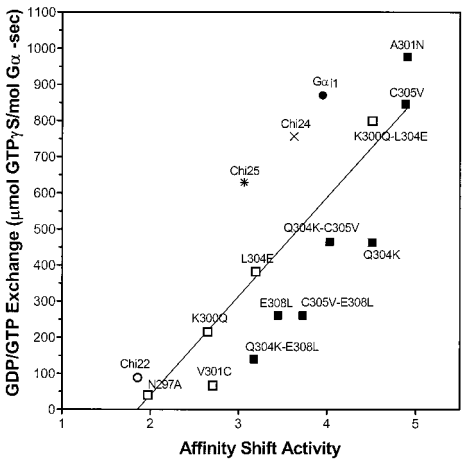

FIG. 7. **Correlation between GDP/GTP exchange and affinity shift activity.** The data plotted represent the means of each data set as reported in Table I. *Filled circle* represents the Gα$_{i1}$ control value; *open circle* represents Chi22; *open squares* represent Chi22 mutants; *filled squares* represent Gα$_{i1}$ mutants. Chi24 is represented by ×, and Chi25 is represented by an *asterisk*. The Pearson correlation coefficient was 0.80, representing a significant correlation between both data sets.

Computer Simulation of Double Point Mutations Reveal Potential for Direct Interaction of Gln^{304} and Glu^{308} with the 5-HT$_{1B}$ Receptor—Whereas the present study demonstrates the critical role of two specific amino acids within the α4 helical domain of Gα$_{i1}$, this mutagenesis approach could not assess whether the 5-HT$_{1B}$ receptor directly interacts with Gln^{304} and Glu^{308} or whether these residues have an indirect effect on receptor coupling as a result of structural changes that occur secondary to amino acid substitution. As shown in Fig. 8, both of these residues are potentially available for direct interaction with the 5-HT$_{1B}$ receptor. In fact, the residues might represent one contact point within a receptor-binding surface which also includes the carboxyl-terminal α-helix of Gα$_{i1}$ and perhaps the β6 strand (Fig. 8). To determine whether the Q304K-E308L mutation could alter the surface electrostatic potential of Gα$_{i1}$, we utilized the GRASP program (developed by A. Nicholls and B. Honig, Columbia University) to compare the mutant α subunit (Gα$_{i1}$-Q304K-E308L) to native Gα$_{i1}$. The net molecular charge of Gα$_{i1}$ is −3, whereas the net charge of the mutant is −1. As shown in Fig. 9*A*, Gα$_{i1}$ residues Gln^{304}, Glu^{308}, and Thr^{321} produce a pocket of negative charge at the surface. The Q304K-E308L mutation of Gα$_{i1}$ changes the surface potential near these residues to a net positive charge. In addition, the surfaces immediately surrounding these residues are now more neutral than in native Gα$_{i1}$. The marked change in the surface potential as a result of these mutations may alter the strength of receptor contact with the α subunit.

Alternatively, rather than affecting direct contact sites with the receptor, the amino acid substitutions within Gα$_{i1}$ may have resulted in secondary structural changes in neighboring domains. The α4–β6 loop region of Gα$_{i1}$ and the β6 strand are possible candidate domains for secondary disruptions consequent to amino acid mutation. The three-dimensional crystal structures of both G$_t$ and Gα$_{i1}$ show that the conformations of the α4 helix and α4–β6 loop are almost identical between these subunits (Fig. 10*A*). Therefore, as the amino acid substitutions that were generated in the present study were substitutions of Gα$_t$ residues for Gα$_{i1}$ residues, it is unlikely that these substitutions would have a marked effect on the secondary structure in this domain. This contention is supported by the fact that all mutant Gα subunits examined in the current study remain capable of full activation by light-activated rhodopsin (data not shown). However, as illustrated in Fig. 10*B*, Gln^{304} of Gα$_{i1}$ forms a hydrogen bond with both the side chain carboxyl groups of Glu^{308} and with the γ hydroxyl group of Thr^{321}. In contrast, Gα$_t$ residue Lys^{300} forms a van der Waals interaction with the δ carbon on Leu^{304}. Substitution of Gα$_{i1}$ residues Gln^{304} and Glu^{308} with the corresponding amino acids from Gα$_t$ (Lys^{300} and Leu^{304}) results in the loss of strong side chain interactions (compare Gα$_i$ and Gα$_t$ contacts in Fig. 10*B*). This suggests that these mutations might weaken the interaction of the α4 helical domain with the β6 strand resulting in an α subunit structure that is less responsive to 5-HT$_{1B}$ receptor-mediated conformational change.

DISCUSSION

By using Gα$_i$/Gα$_t$ chimeras and site-directed mutagenesis, the present study determined that two residues (Gln^{304} and Glu^{308}) within the α4 helical domain of Gα$_{i1}$ are required for 5-HT$_{1B}$ receptor coupling to Gα$_{i1}$. These results are consistent with our previous work implicating the α4 helix and α4—β6 loop region of Gα$_{i1}$ in 5-HT$_{1B}$ receptor coupling to inhibitory G proteins. Taken together, these studies provide evidence for a previously unappreciated role for the α4 helix of α subunits in directing G protein-coupled receptor interactions.

Previously published work has shown that there are several receptor-binding regions present in heterotrimeric G proteins. The primary receptor recognition region is believed to be localized to the carboxyl-terminal domain of Gα subunits (13–18), although at least three other regions in Gα are involved in receptor interaction: the amino-terminal domain (18, 20, 41); the α2 helix and α2-β4 loop regions (16, 19); and the α4 helix and α4-β6 loop domain (1, 16, 42). In addition, segments of the β and γ subunits may contribute to the receptor interacting surface of heterotrimers (20–25). Whether individual G protein-coupled receptors interact simultaneously with several regions on heterotrimers and/or whether the profile of physical contacts for a particular receptor may direct more subtle features of specificity such as the efficiency of receptor coupling remains to be determined.

Other studies implicating the α4 helix and/or α4–β6 loop regions of Gα in receptor interactions include studies from alanine scanning mutagenesis on Gα$_t$ (16), patterns of evolutionary conservation (43), and tryptic digestion of Gα$_t$ bound to rhodopsin (42). Interestingly, the recently resolved crystal structure of Gα$_s$ by Sunahara *et al*. (44) indicates that although the overall structures of Gα$_s$ and Gα$_i$ are quite similar, the α4 helix and α4-β6 loop region varies between these subunits both in the length of the helical domain and the positioning of this region within the molecule itself (44). Thus the sequence divergence and structural differences between these Gα's is consistent with an important role in specific receptor recognition.

According to the crystal structure of Gα$_i$ (30), in three-dimensional space Gln^{304} and Glu^{308} are situated on the same molecular surface as the carboxyl-terminal tail of the Gα subunit which has been well established as a receptor-binding site (Fig. 8). The α4 helix is connected to the carboxyl-terminal domain via the α4-β6 loop, followed by the β6 strand and the β6–α5 loop which contains a conserved guanine nucleotide binding motif TCAT (Fig. 10*A*). Several biochemical studies have reported that mutations within this TCAT motif dramatically decrease the affinity of the α subunit for GDP (16, 45, 46). Therefore, one could hypothesize that the 5-HT$_{1B}$ receptor interaction with both the α4 helical domain and the carboxyl-terminal region might trigger changes in the β6–α5 loop. Upon agonist activation of the receptor, both domains may translate a conformational change to the TCAT motif resulting in a lowered affinity of GDP for the nucleotide binding pocket. Key mutations within either one of these domains (*i.e.* the α4 helix or carboxyl terminus) may alter the transmission of the recep-

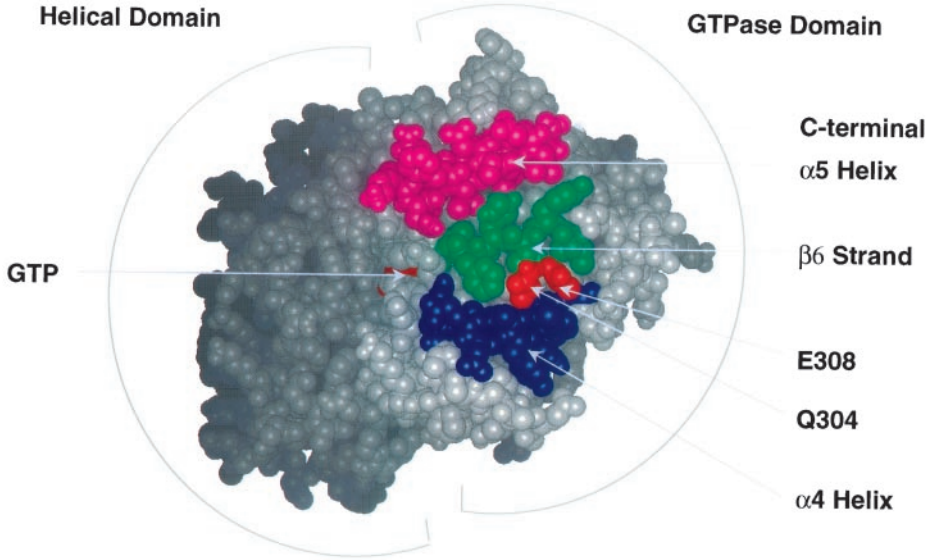

FIG. 8. **Space filling model of the GTP bound form of $G\alpha_{i1}$ highlighting both known and hypothetical receptor contact sites on the $G\alpha$ subunit.** Residues within the α4 helical domain (*purple*), which were determined to be critical for 5-HT_{1B} receptor coupling (Gln^{304} and Glu^{308}), are colored *orange* to illustrate that these residues are surface-exposed and could potentially directly interact with the 5-HT_{1B} receptor. A hypothetical receptor-binding site may also include portions of the β6 strand (*green*) as well as the α5 helical-carboxyl-terminal domain (*fuchsia*). The guanine nucleotide (*orange*) is shown buried within the core of the α subunit. The model was generated using INSIGHT II (Biosym Technologies, San Diego, CA) with the crystal structure coordinates from (30).

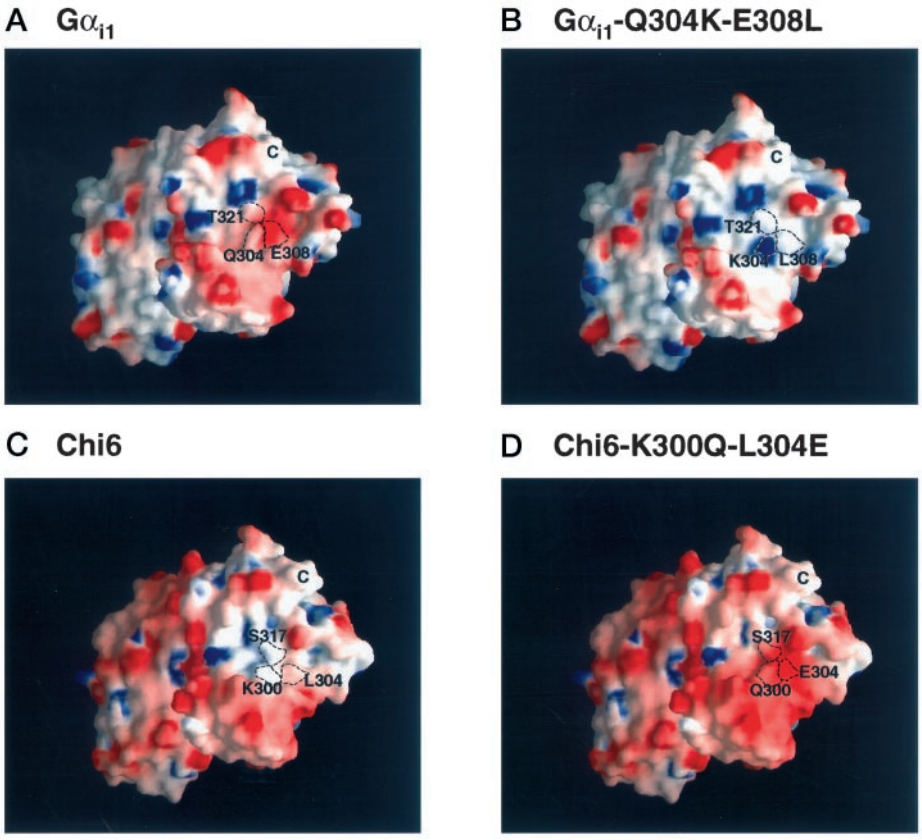

FIG. 9. **Solvent-accessible surface of α subunits colored according to the electrostatic potential.** The solvent-accessible surface of GTPγS-bound $G\alpha_{i1}$ (30) and GDP-bound Chi6 (51) are shown in *A* and *C*, respectively. Using INSIGHT II (version 2.3.0 Viewer Module), computer-simulated models of the crystal structures of $G\alpha_{i1}$-Q304K-E308L and Chi6-K300Q-L304E were generated. The solvent-accessible surfaces of these mutants were then calculated using the GRASP program (developed by A. Nicholls and B. Honig, Columbia University). These models simulate the impact of the double mutation on the surface electrostatic potential of the α subunit. The electrostatic potential is contoured in the range from $-10k_BT$ (*red*) to $+10\ k_BT$ (*blue*) where k_B is Boltzmann's constant and T is the absolute temperature (K). Amino acids are labeled based on their relative sequence positions (30, 31, 51, 52). *C,* carboxyl terminus.

tor-induced conformational signal to the TCAT domain and result in an inability to release GDP upon agonist binding.

Consistent with this idea, it has been suggested that the agonist-activated receptor interacts with the GDP-bound form of the heterotrimeric G protein, and the release of GDP from the Gα subunit is the rate-limiting step in G protein activation (47–49). This guanine nucleotide free form of the G protein exists in a highly stable complex with the agonist-bound receptor in the absence of guanine nucleotides in the medium (50). Therefore, mutations of $G\alpha_i$ that generate defects in agonist-activated receptor-catalyzed GDP release from the Gα subunit should also result in a failure to establish the high affinity ternary complex of agonist, receptor, and G protein. In fact, as shown in Fig. 7, a good overall correlation does exist between the two measurements of GTPγS binding and affinity shift activity.

Sequence alignment and comparison of the primary structure between $G\alpha_{i/o}$ family members reveals that α4 helical residues Gln^{304} and Glu^{308} are absolutely conserved among the members of the $G_{i/o}$ family of α subunits shown in Fig. 11. In contrast, residues in the homologous position on $G\alpha_t$ are different. The conservation of these critical residues across $G\alpha_{i1}$, $G\alpha_{i2}$, $G\alpha_{i3}$, and $G\alpha_o$ members of the $G_{i/o}$ family is consistent with the ability of the 5-HT_{1B} receptor to couple selectively to heterotrimers containing any one of these members within this family of α subunits (12). These data are also consistent with published studies indicating that the 5-HT_{1B} receptor is incapable of coupling to heterotrimers containing $G\alpha_t$ (1, 12).

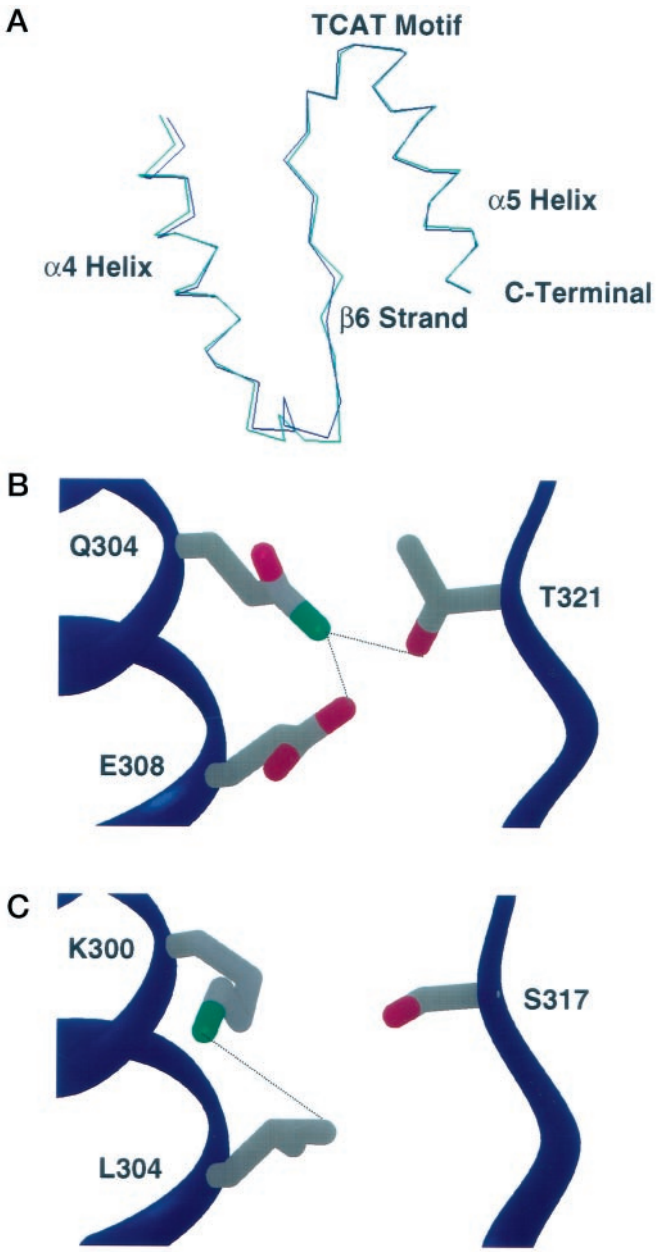

FIG. 10. **Secondary structure and residue contact sites in $G\alpha_{i1}$ and $G\alpha_t$.** Superimposed Cα traces of α4 helix through carboxyl-terminal residues (*A*) of free $G\alpha_i$-GTP (*green*) and $G\alpha_t$-GTP (*blue*). This overlay demonstrates that there is little difference between the secondary structure of $G\alpha_i$ and $G\alpha_t$ within this domain. In addition, the TCAT motif is "linked" to the carboxyl-terminal domain via the α5 helix and to the α4 helix via the β6 strand followed by the α4–β6 loop. *Ribbon* representation of portions of the α4 helix and β6 strand of free $G\alpha_{i1}$-GTP (*B*) and $G\alpha_t$-GTP (*C*). The side chains from $G\alpha_{i1}$ residues Gln^{304}, Glu^{308}, and Thr^{321} in addition to $G\alpha_t$ residues Lys^{300}, Lys^{304}, and Ser^{317} are drawn as stick models to illustrate physical contacts of critical residues. *Fuchsia* residues represent oxygen atoms, and *green* residues represent nitrogen atoms. *Dashed lines* indicate intramolecular contacts between residues. Amino acids are labeled based on their respective sequence positions (30, 52). The GTP-bound α subunits are illustrated because the GDP-bound form of $G\alpha_i$ contains a microdomain that changes the conformation of the carboxyl terminus.

Clawges *et al*. (12) demonstrated that whereas G_{i1}, G_{i2}, G_{i3}, or G_o can couple to the 5-HT_{1B} receptor, these subunits exhibited a rank order profile of coupling efficiency ($G_{i3} \approx G_{i1} > G_o > G_{i2}$) to the receptor. Together, the current data and previously published work suggest that residues other than those identified within the α4 helical domain may mediate more subtle differences in coupling efficiency between G proteins within the same subfamily.

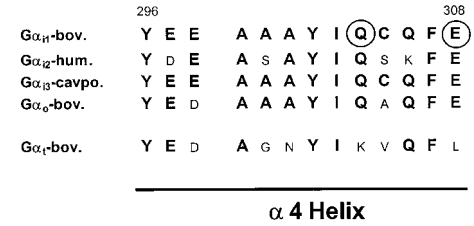

FIG. 11. **Primary sequence alignment of α4 helical region of Gα subunits.** *Numbers above* the sequences refer to amino acid positions in the context of $G\alpha_{i1}$. *Boldface letters* represent identical amino acid residues among $G\alpha_{i/o}$ subunits. The *circled* amino acid residues in $G\alpha_{i1}$ are those that were determined to be critical for 5-HT_{1B} receptor coupling. Notice that these amino acids are conserved among several members of the $G\alpha_{i/o}$ family of α subunits but diverge from the corresponding residues in $G\alpha_t$. *bov.*, bovine; *hum.*, human; *cavpo.*, guinea pig.

In summary, 2 amino acids within the α4 helix of the Gα subunit play a key role in directing the specificity of 5-HT_{1B} receptor coupling. These residues are essential for ensuring both the formation of the high affinity state of the receptor in the presence of agonist and receptor-catalyzed GDP/GTP exchange. Conservation of these residues across several members of the $G_{i/o}$ family of α subunits strengthens the importance of these residues in agonist G protein activation and suggests that other receptors that distinguish between $G\alpha_i$ and $G\alpha_t$ may utilize these residues as well. It remains to be determined whether these residues interact directly with the receptor or act indirectly by affecting the secondary structure of Gα or the transmission of conformational changes to the GDP-binding pocket. Future work on the generalizability of these results to other G_i-coupled receptors will contribute to the understanding of the mechanism of receptor-catalyzed G protein activation and the nature of selectivity governing various cellular responses elicited by different biological stimuli.

Acknowledgments—We gratefully acknowledge Dr. Maria Mazzoni and Tarita Thomas for critically reading the manuscript and for providing editorial assistance. We also thank Drs. Tohru Kozasa and Alfred G. Gilman for kindly providing the baculovirus expressing His_6-γ_2.

REFERENCES

1. Bae, H., Anderson, K., Flood, L. A., Skiba, N. P., Hamm, H. E., and Graber, S. G. (1997) *J. Biol. Chem.* **272,** 32071–32077
2. Conklin, B. R., and Bourne, H. R. (1993) *Cell* **73,** 631–641
3. Neer, E. J. (1995) *Cell* **80,** 249–257
4. Hamm, H. E., and Gilchrist, A. (1996) *Curr. Opin. Cell Biol.* **8,** 189–196
5. Munshi, R., Pang, I. H., Sternweis, P. C., and Linden, J. (1991) *J. Biol. Chem.* **266,** 22285–22289
6. Raymond, J. R., Olsen, C. L., and Gettys, T. W. (1993) *Biochemistry* **32,** 11064–11073
7. Kurose, H., Regan, J. W., Caron, M. G., and Lefkowitz, R. J. (1991) *Biochemistry* **30,** 3335–3341
8. Migeon, J. C., and Nathanson, N. M. (1994) *J. Biol. Chem.* **269,** 9767–9773
9. Laugwitz, K. L., Offermanns, S., Spicher, K., and Schultz, G. (1993) *Neuron* **10,** 233–242
10. Kubota, A., Yamada, Y., Kagimoto, S., Yasuda, K., Someya, Y., Ihara, Y., Okamoto, Y., Kozasa, T., Seino, S., and Seino, Y. (1994) *Biochem. Biophys. Res. Commun.* **204,** 176–186
11. Gudermann, T., Kalkbrenner, F., and Schultz, G. (1996) *Annu. Rev. Pharmacol. Toxicol.* **36,** 429–459
12. Clawges, H. M., Depree, K. M., Parker, E. M., and Graber, S. G. (1997) *Biochemistry* **36,** 12930–12938
13. Conklin, B. R., Farfel, Z., Lustig, K. D., Julius, D., and Bourne, H. R. (1993) *Nature* **363,** 274–276
14. Liu, J., Conklin, B. R., Blin, N., Yun, J., and Wess, J. (1995) *Proc. Natl. Acad. Sci. U. S. A.* **92,** 11642–11642
15. Kostenis, E., Conklin, B. R., and Wess, J. (1997) *Biochemistry* **36,** 1487–1495
16. Onrust, R., Herzmark, P., Chi, P., Garcia, P. D., Lichtarge, O., Kingsley, C., and Bourne, H. R. (1997) *Science* **275,** 381–384
17. Rasenick, M. M., Watanabe, M., Lazarevic, M. B., Hatta, S., and Hamm, H. E. (1994) *J. Biol. Chem.* **269,** 21519–21525
18. Hamm, H. E., Deretic, D., Arendt, A., Hargrave, P. A., Koenig, B., and Hofmann, K. P. (1988) *Science* **241,** 832–835
19. Lee, C. H., Katz, A., and Simon, M. I. (1995) *Mol. Pharmacol.* **47,** 218–223
20. Taylor, J. M., Jacob-Mosier, G. G., Lawton, R. G., Remmers, A. E., and Neubig, R. R. (1994) *J. Biol. Chem.* **269,** 27618–27624

21. Taylor, J. M., Jacob-Mosier, G. G., Lawton, R. G., VanDort, M., and Neubig, R. R. (1996) *J. Biol. Chem.* **271,** 3336–3339
22. Kisselev, O., Pronin, A., Ermolaeva, M., and Gautam, N. (1995) *Proc. Natl. Acad. Sci. U. S. A.* **92,** 9102–9106
23. Kisselev, O., Ermolaeva, M., and Gautam, N. (1995) *J. Biol. Chem.* **270,** 25356–25358
24. Kisselev, O., Ermolaeva, M. V., and Gautam, N. (1994) *J. Biol. Chem.* **269,** 21399–21402
25. Yasuda, H., Lindorfer, M. A., Woodfork, K. A., Fletcher, J. E., and Garrison, J. C. (1996) *J. Biol. Chem.* **271,** 18588–18595
26. Engel, G., Gothert, M., Hoyer, D., Schlicker, E., and Hillenbrand, K. (1986) *Naunyn-Schmidedbergs Arch. Pharmakol.* **332,** 1–7
27. Hamblin, M. W., and Metcalf, M. A. (1991) *Mol. Pharmacol.* **40,** 143–148
28. Middlemiss, D. N., Bremer, M. E., and Smith, S. M. (1988) *Eur. J. Pharmacol.* **157,** 101–107
29. Goadsby, P. J. (1998) *Clin. Neurosci.* **5,** 18–23
30. Coleman, D. E., Berghuis, A. M., Lee, E., Linder, M. E., Gilman, A. G., and Sprang, S. R. (1994) *Science* **265,** 1405–1412
31. Wall, M. A., Coleman, D. E., Lee, E., Iniguez-Lluhi, J. A., Posner, B. A., Gilman, A. G., and Sprang, S. R. (1995) *Cell* **83,** 1047–1058
32. Skiba, N. P., Bae, H., and Hamm, H. E. (1996) *J. Biol. Chem.* **271,** 413–424
33. Bradford, M. M. (1976) *Anal. Biochem.* **72,** 248–254
34. Graber, S. G., Figler, R. A., and Garrison, J. C. (1992) *J. Biol. Chem.* **267,** 1271–1278
35. Boyer, J. L., Graber, S. G., Waldo, G. L., Harden, T. K., and Garrison, J. C. (1994) *J. Biol. Chem.* **269,** 2814–2819
36. Kozasa, T., and Gilman, A. G. (1995) *J. Biol. Chem.* **270,** 1734–1741
37. Mazzoni, M. R., Malinski, J. A., and Hamm, H. E. (1991) *J. Biol. Chem.* **266,** 14072–14081
38. Figler, R. A., Graber, S. G., Lindorfer, M. A., Yasuda, H., Linden, J., and Garrison, J. C. (1996) *Mol. Pharmacol.* **50,** 1587–1595
39. Asano, T., Ui, M., and Ogasawara, N. (1985) *J. Biol. Chem.* **260,** 12653–12658
40. Pobiner, B. F., Northup, J. K., Bauer, P. H., Fraser, E. D., and Garrison, J. C. (1991) *Mol. Pharmacol.* **40,** 156–167
41. Kostenis, E., Degtyarev, M. Y., Conklin, B. R., and Wess, J. (1997) *J. Biol. Chem.* **272,** 19107–19110
42. Mazzoni, M. R., and Hamm, H. E. (1996) *J. Biol. Chem.* **271,** 30034–30040
43. Lichtarge, O., Bourne, H. R., and Cohen, F. E. (1996) *Proc. Natl. Acad. Sci. U. S. A.* **93,** 7507–7511
44. Sunahara, R. K., Tesmer, J. J., Gilman, A. G., and Sprang, S. R. (1997) *Science* **278,** 1943–1947
45. Garcia, P. D., Onrust, R., Bell, S. M., Sakmar, T. P., and Bourne, H. R. (1995) *EMBO J.* **14,** 4460–4469
46. Thomas, T. C., Schmidt, C. J., and Neer, E. J. (1993) *Proc. Natl. Acad. Sci. U. S. A.* **90,** 10295–10298
47. Wess, J. (1997) *FASEB J.* **11,** 346–354
48. Bourne, H. R. (1997) *Curr. Opin. Cell Biol.* **9,** 134–142
49. Ferguson, K. M., Higashijima, T., Smigel, M. D., and Gilman, A. G. (1986) *J. Biol. Chem.* **261,** 7393–7399
50. Bornancin, F., Pfister, C., and Chabre, M. (1989) *Eur. J. Biochem.* **184,** 687–698
51. Lambright, D. G., Sondek, J., Bohm, A., Skiba, N. P., Hamm, H. E., and Sigler, P. B. (1996) *Nature* **379,** 311–319
52. Noel, J. P., Hamm, H. E., and Sigler, P. B. (1993) *Nature* **366,** 654–663